

Formation and Properties of Selenium Double-Helices inside Double-Wall Carbon Nanotubes: Experiment and Theory

Toshihiko Fujimori,[†] Renato Batista dos Santos,^{‡,§} Takuya Hayashi,[⊥] Morinobu Endo,[†] Katsumi Kaneko,[†]
and David Tománek^{*,§}

[†]Research Center for Exotic Nanocarbons (JST), Shinshu University, 4-17-1 Wakasato, Nagano-city 380-8553, Japan

[‡]Universidade Federal da Bahia, Instituto de Física, Salvador, Bahia 40.210-340, Brazil

[§]Physics and Astronomy Department, Michigan State University, East Lansing, Michigan 48824, USA

[⊥]Faculty of Engineering, Shinshu University, 4-17-1 Wakasato, Nagano-city 380-8553 Japan

*tomanek@pa.msu.edu

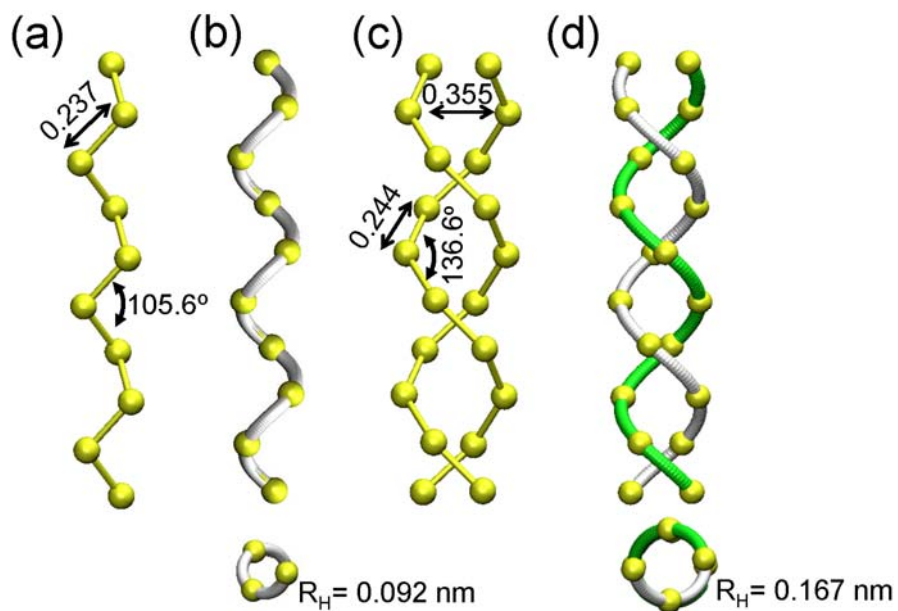


Figure S1. Helical structures of Se investigated theoretically in our study. (a) Optimized geometry and (b) model of a Se single-helix structure. (c) Optimized geometry and (d) model of a Se double-helix structure. Distances are given in nm units.

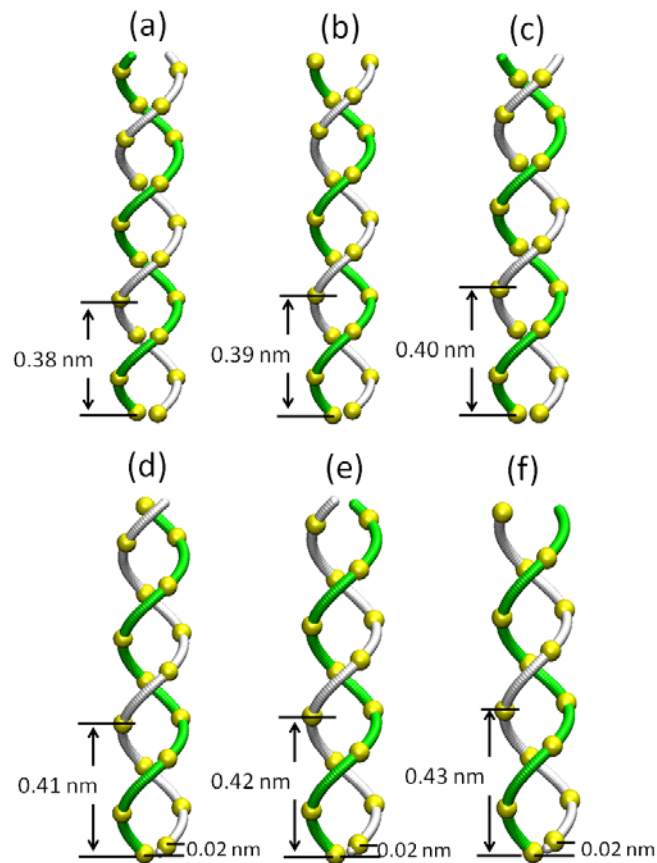


Figure S2. Optimized structures of free Se double-helices subject to changes in the axial unit cell size. (a) $a_3=0.38$ nm, (b) $a_3=0.39$ nm, (c) $a_3=0.40$ nm, (d) $a_3=0.41$ nm, (e) $a_3=0.42$ nm; (f) $a_3=0.38$ nm. Strands of double-helix structures with long unit cells undergo a small axial offset.

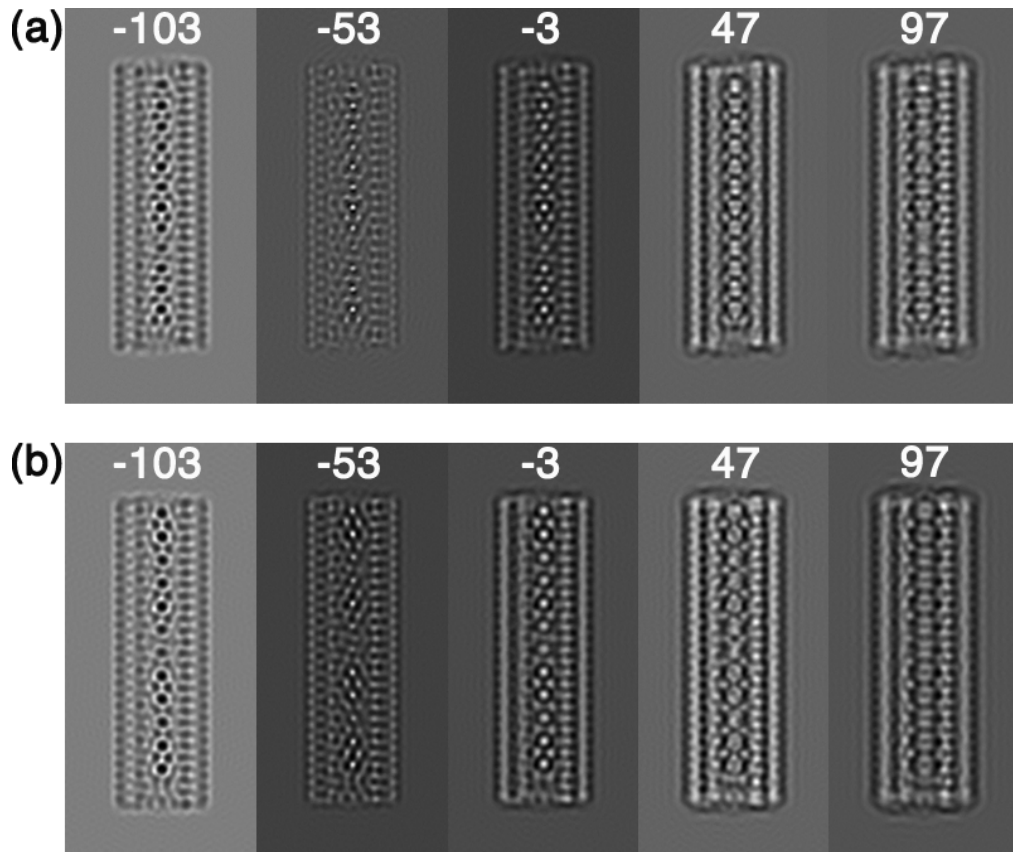


Figure S3. Simulated TEM images of Se double-helices, shown in Figure 3(a) of the main manuscript, for -103 to 97 nm defocus condition (Scherzer defocus condition: -53 nm). Simulations are performed for two representative geometries of Figure S2: (a) $a_3=0.38$ nm and (b) $a_3=0.43$ nm.

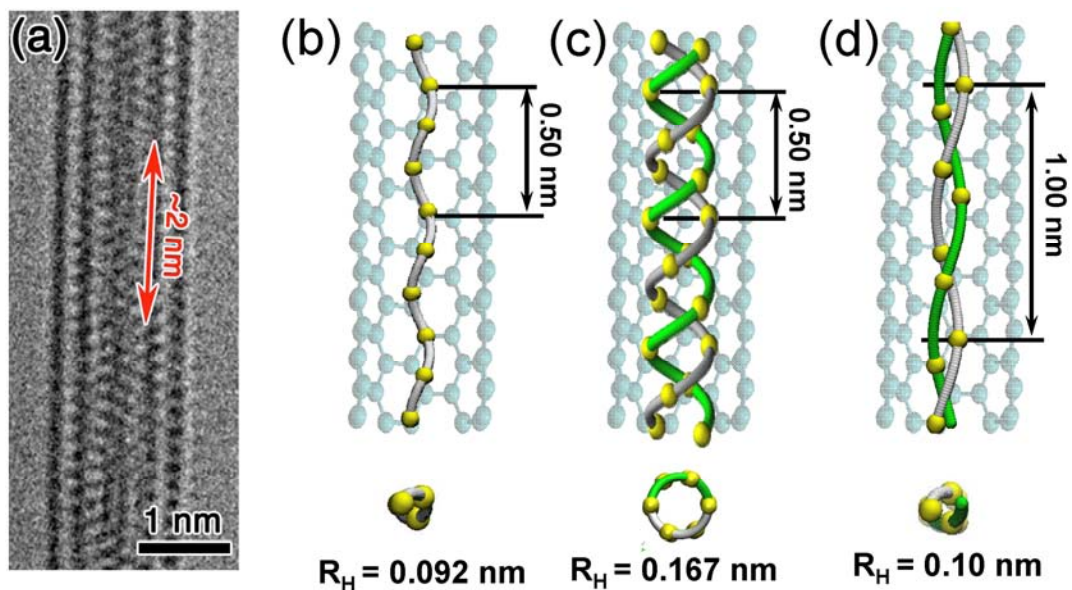


Figure S4. (a) TEM image of a Se helix with a pitch length of 2 nm confined in a DWCNT. (b) Se single-helix with a pitch length of 0.5 nm inside a (5,5) carbon nanotube. (c) Se double-helix with a pitch length of 0.5 nm inside a (5,5) carbon nanotube. (d) Se double-helix with a severely reduced helix radius R_H and a large pitch length of 1.0 nm inside a (5,5) carbon nanotube.

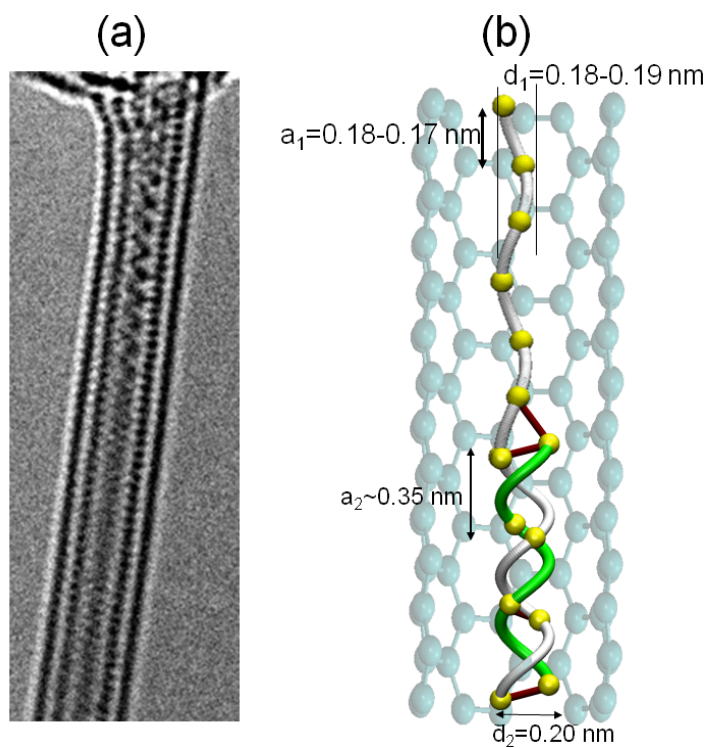


Figure S5. (a) TEM image of a Se single-helix connected to a Se double-helix inside a DWCNT, reproduced from Figure 3(c) of the main manuscript. (b) Structural model representing the optimized geometry.

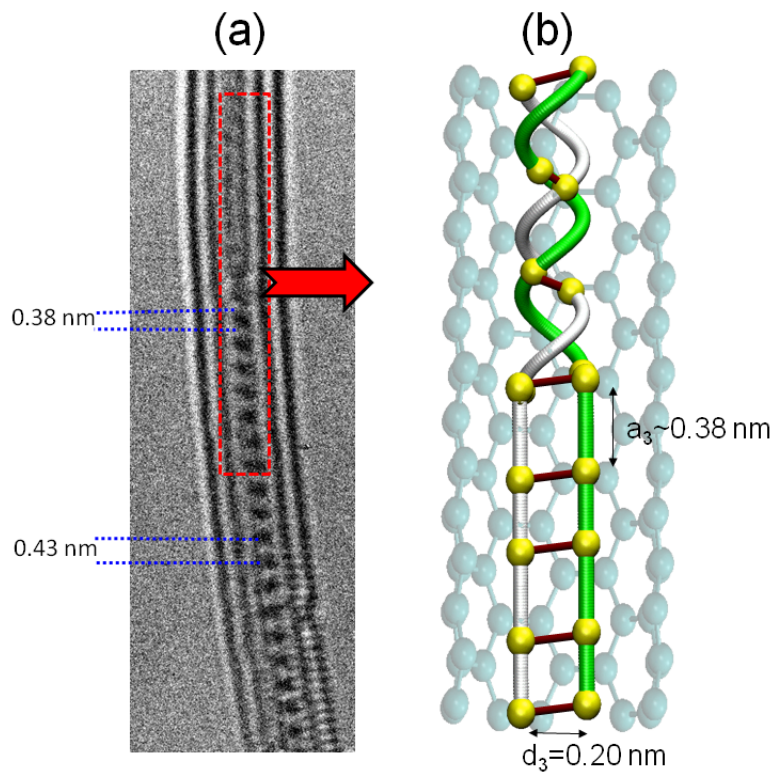
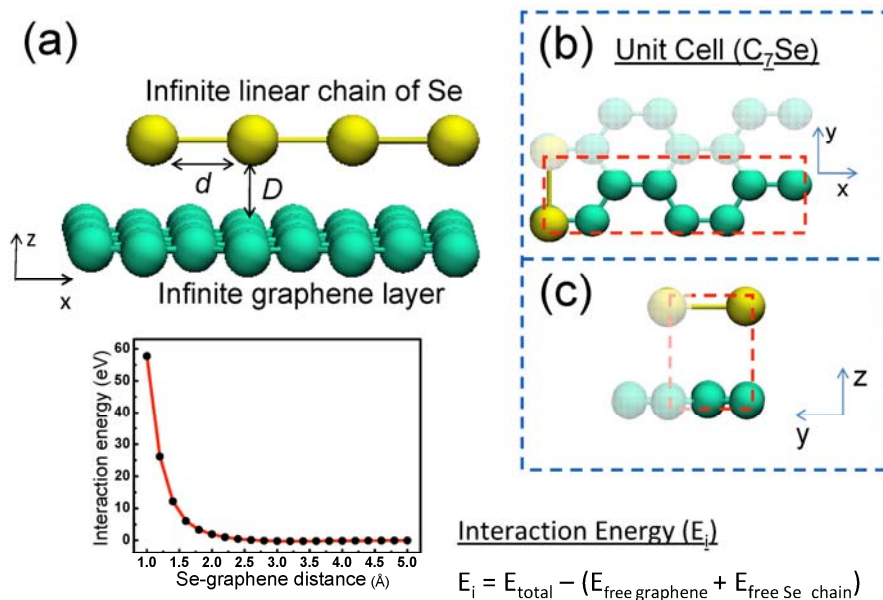


Figure S6. (a) TEM image of a Se double-helix structure connected to a linear Se ladder structure inside a DWCNT. (b) Structural model representing the optimized geometry.



d : Se-Se distance

D : distance between the Se chain and graphene

Figure S7. Interaction between an infinite graphene layer and an infinitely long linear Se chain. (a) Perspective view of the structure and interaction energy as a function of the Se-graphene separation. The C_7Se unit cell used in the calculation in the (b) xy plane and (c) yz plane.

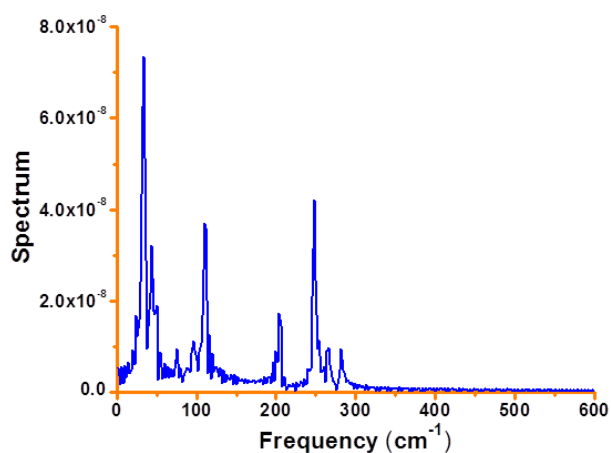


Figure S8. Vibration spectrum of a free Se helix obtained from the analysis of the velocity-velocity autocorrelation function obtained during a microcanonical molecular dynamics simulation.

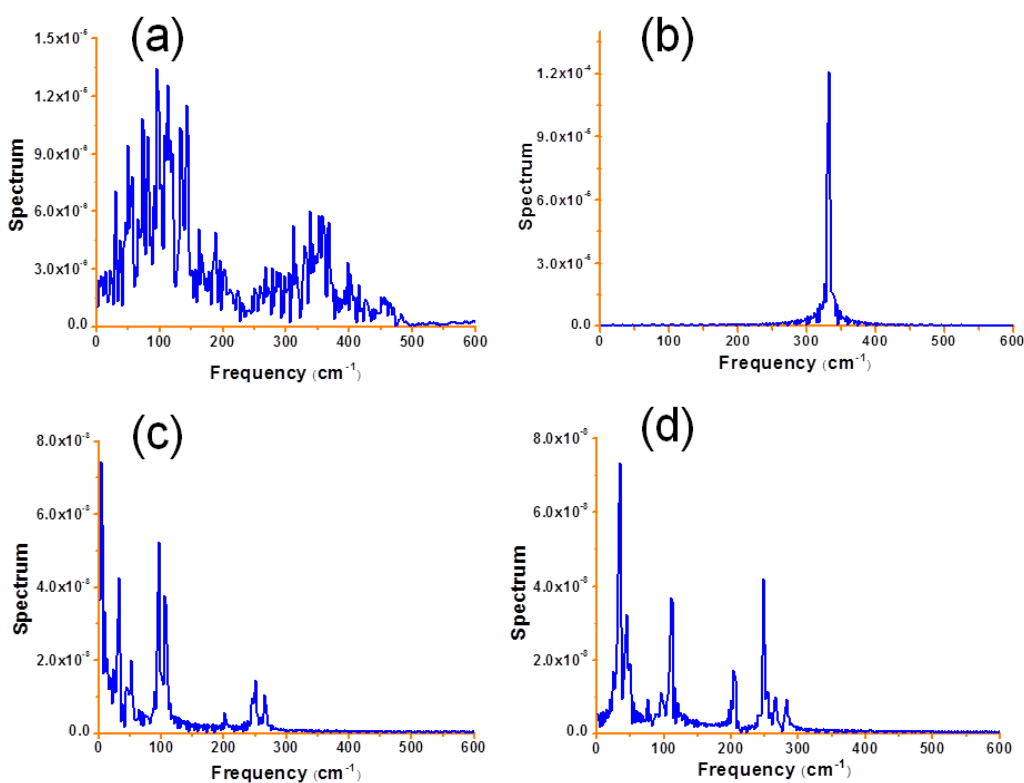


Figure S9. Vibration spectra of Se helices confined in cylindrical cavities with different radii, obtained using microcanonical molecular dynamics simulations. The diameters of the cavities that represent enclosing nanotubes were (a) $d=0.44$ nm, (b) $d=0.64$ nm, (c) $d=0.84$ nm, and (d) $d=1.04$ nm.

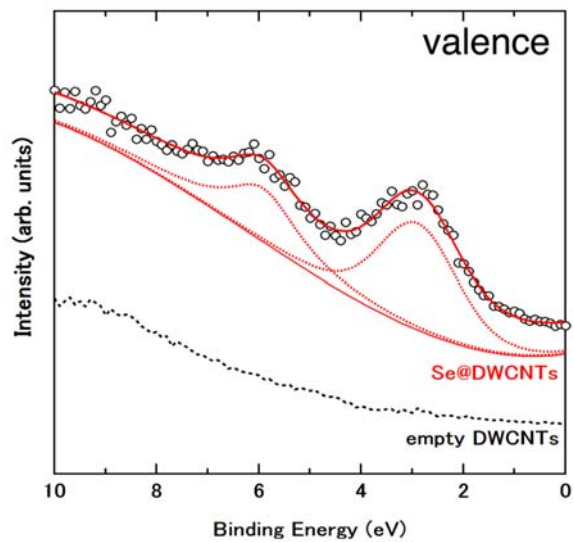


Figure S10. XPS valence-state spectra of Se@DWCNTs, shown by the red solid line, in comparison to spectra of empty DWCNTs, shown by the black dotted line. The two peaks at 2.9 and 5.9 eV below the Fermi level at $E=0$ resemble the density of states in Figures 6(a) and (b) of the main article and can be attributed to the helical structure of Se.

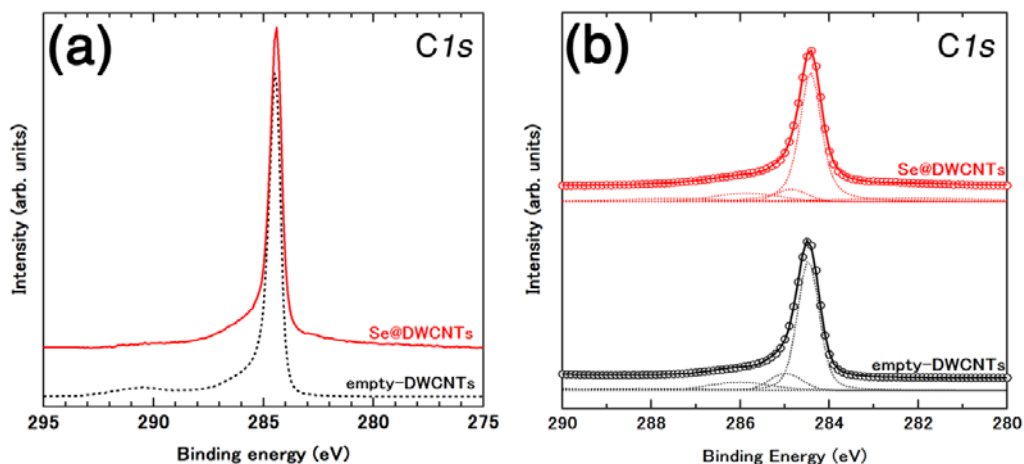


Figure S11. (a) Comparison between XPS $C1s$ spectra of Se@DWCNTs (red solid line) and empty DWCNTs (black dotted line). (b) XPS spectra of Se@DWCNTs (red open circles) and empty DWCNTs (black open circles), fitted with the Voigt function. The background was subtracted using the Shirley equation, which is commonly used for removing the background of XPS spectra. Both Se@DWCNTs and empty DWCNTs show an intense $C1s$ peak at 284.5 eV, which originates from sp^2 -bonded carbon atoms. Since the $C1s$ spectra of empty DWCNTs and Se@DWCNTs are almost identical, we conclude that charge transfer and/or chemical bonding between inner CNTs and the Se double-helices are negligible. We note that the intensities of sub-bands associated with sp^3 -bonded carbon atoms at 284.9 eV and with C-O functional group at 285.9 eV are slightly lower in Se@DWCNTs than in pristine DWCNTs due to the removal of the C-O functional groups during the encapsulation process of Se, which occurs at high temperatures ($T=973$ K) under vacuum conditions.

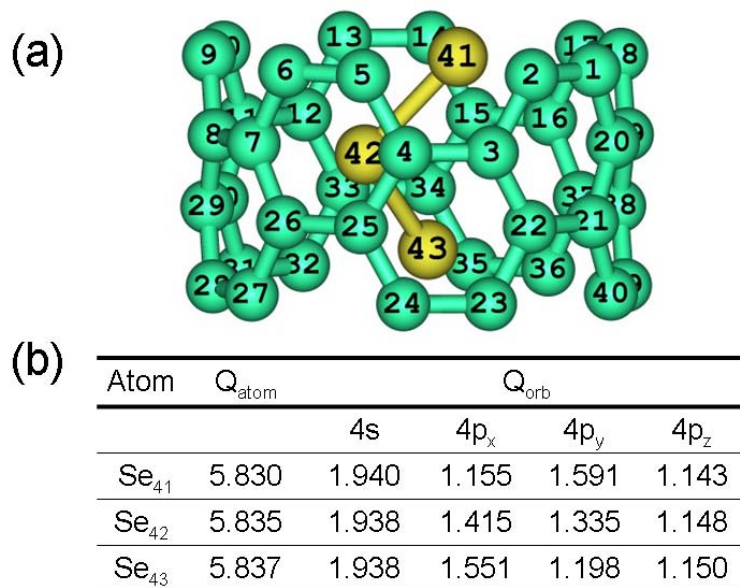


Figure S12. Mulliken population analysis of a Se helix confined in a (5,5) carbon nanotube. (a) Atomic arrangement in the unit cell of the system. Carbon atoms, shown in green, carry labels 1-40, and Se atoms, shown in yellow, carry labels 41-43. (b) Net valence charge Q_{atom} , as well as its components Q_{orb} for the different orbitals, are presented for the Se atoms.